J. Mountain Res. P-ISSN: 0974-3030, E-ISSN: 2582-5011
Vol. 21(S2), (2026) 104-112
DOI: https://doi.org/10.51220/jmr.v21-S2.13

Influence of strontium (Sr) content on the structural and ferroelectric characteristics of lead-free $(Ba_{1-x}Sr_xCa_{0.1})(Zr_{1-z}Ti_z)O_3$ (x = 0.20, z = 0.9) ceramics

Don Biswas[1*] • Surendra Singh[2] • Manish Uniyal[3] • N. S. Panwar[1]

[1] *Department of Instrumentation Engineering, H.N.B.G.U, Srinagar (Garhwal), Uttarakhand, India*
[2] *Department of Sciences (Physics) Quantum University, Roorkee, Uttarakhand, India.*
[3] *Department of Physics, H.N.B.G.U, Srinagar (Garhwal), Uttarakhand, India*

*Corresponding Author's Email Id: donusic06@gmail.com

Received: 20.02.2025; Revised: 30.10.2025; Accepted: 19.11.2025

Abstract: The influence of strontium (Sr) on the phase structure, microstructure, dielectric, and piezoelectric properties of the $(Ba_{1-x}Sr_xCa_{0.1})(Zr_{1-z}Ti_z)O_3$ (x = 0.20, z = 0.9) sintered pellet sample have been studied. The structural and piezoelectric characteristics of the synthesized BSCZT sample have also been explored at RT. The dielectric characteristics (ε, tan δ, and σ) of the synthesized composition were observed over a wide choice of temperature (from RT to 450 °C) and frequencies (12.74-1000 kHz). SEM photographs were taken at room temperature (RT). The density and grain size were measured. The selected composition may give enhanced results compared to the BCZT ceramics. Therefore, lead-free BSCZT composition could be an ideal candidate for a range of electrical applications.

Keywords: Morphotropic phase boundary • XRD • SEM • dielectric constant • electric conductivity.

Introduction

The remarkable electrical and optical properties of dielectric compounds with perovskite ABO_3-type symmetry make them highly significant for technological applications (Samara 1987). Lead-free dielectric materials show great potential for use in actuators and various sensors owing to their excellent ferroelectric properties (Samara 1987). $BaTiO_3$ has become one of the most researched and promising perovskite ceramics with ABO_3 symmetry in this particular area (Wu J et al., 2012, Jiang M et al., 2013). Three consecutive phase transitions - from cubic to tetragonal structure at 393 K, from tetragonal to orthorhombic structure at 298 K, and from orthorhombic to rhombohedral structure at 183 K- are what make $BaTiO_3$ ceramics important (Takenaka T et al., 2005). By substituting the "A- and/or B-site" atoms with atoms that have the right valence and tolerance, a variety of binary and ternary perovskite solid mixtures may be synthesized. A promising alternative to ceramics containing lead across a range of ferroelectric and dielectric utilization is the BSCZT ("barium strontium calcium zirconate Titanate") system, which is a subset of these ferroelectric compounds (Saito Y et al., 2004, Dawber M et al., 2005, Kantha P et al., 2009). Any value of x (x = 0 to 0.9) can be used to create solid solutions of the $(Ba_{0.9-x}Sr_xCa_{0.1})(Zr_{0.1}Ti_{0.9})O_3$ ceramics, enabling a great deal of electrical characteristics customization. By replacing Ba with Sr, Ca with Zr, and Ti with Zr, the BSCZT system can be altered to produce binary solid solutions. The Curie temperature (T_c) somewhat changes when Ca^{2+} ions are used to replace the A-site. On the other hand, the structure changes from ferroelectric to paraelectric when strontium ions (Sr^{2+}) are substituted for calcium ions (Ca^{2+}), and the relative permittivity increases (Kim S et al., 2013, Srinivas A et al., 2015). Additionally, adding Zr^{4+} ions at the Ti- site improves the ferroelectric and dielectric characteristics while lowering the leakage current characteristics (Sateesh P et al., 2015, Chao X et al., 2016). According to Puli et al., energy storage capabilities of these kinds of materials used in ternary ceramics may be improved by the incorporation of strontium (Sr^{2+}) and calcium ions (Ca^{2+}) at the A- site (Puli V S et al., 2014). Bahri et al. explored the dielectric characteristics of the BSCZT samples and discovered that the relaxor behavior grew more noticeably when the quantity of Sr^{2+} ions at A-site raised (Bahri F et al., 2014). The relative permittivity (K) of the BCZT compositions may be raised by altering the quantity of Zr and Ca at the Ti and Ba sites, respectively, according to (Maraj et al. 2014). They also recommended that the BCZT ceramics may be doped with donor and acceptor ions to enhance their piezoelectric characteristics. In the case of BCZT samples, Biswas et al. discovered significant results close to MPB or the morphotropic phase boundary (Biswas D et al. 2021). There are multiple potential phases that can make up an MPB. Different polarization orientations may be initiated by a mixture of these phases, which would explain the obtained dielectric character for the samples close to MPB. Elastic softening of the lattice, intermediate phase presence, and polarization extension and rotation are the reasons for the large piezoelectricity in BSCZT and NKN ceramics at the MPB (Bahri F et al., 2014, Maraj et al. 2014, Biswas D et al. 2021). As a result, there are multiple potential polarization directions in an MPB with both phases, which could lead to a high k_s. It is commonly known that a large dielectric constant is caused by polarization, which is approximately proportional to the size of the atomic displacement. The dielectric and piezoelectric characteristics at MPB depend on composition rather than temperature and frequency (Biswas D et al. 2021). Further, Compared to the base compound barium titanate ($BaTiO_3$), the incorporation of strontium (Sr) into the BCZT system leads to the formation of the BSCZT system, which enhances its dielectric and piezoelectric properties (Kim S et al., 2013, Srinivas A et al., 2015, Puli V S et al., 2014, Liu X et al., 2015). In the current study, the solid-state reaction technique was utilized to synthesize the composition $(Ba_{1-x}Sr_xCa_{0.1})(Zr_{1-z}Ti_z)O_3$ (x = 0.20, z = 0.9). The dielectric properties ("ε, tan δ, and σ") of the synthesized sample were obtained at various frequencies (12.74 to 1000 kHz) and temperatures (RT to 450 °C). At RT, the composition was taken to measure the piezoelectric characteristics. The synthesized composition was also analyzed using scanning electron microscopy (SEM) and X-ray diffraction (XRD) at RT. The observed outcomes highlight the various key properties of the prepared pellet sample, along with their potential applications in sensors and transducers.

Experimental details

The raw materials used in this investigation were high purity (> 99.9%) barium carbonate ($BaCO_3$), calcium carbonate ($CaCO_3$), strontium titanate ($SrTiO_3$), zirconium oxide (ZrO_2) and titanium oxide (TiO_2). A solid-state reaction process was utilized to create the BSCZT ceramics (Biswas D et al. 2021). To get rid of any dissolved moisture, the raw powders were first dried for two hours at 200 °C. The composition of BSCZT system was then prepared by weighing the powders in the stoichiometric ratio, with x = 0.20. With the help of an agate mullet mortar and pestle, the powder was manually dry mixed, grounded for four hrs, and further ground with methanol for two more hrs. The next step is to remove the carbon dioxide. Now, the pulverized powder was calcined at 1200 °C in a muffle furnace. The calcined powder was weighed once it had cooled to room temperature to make sure all of the carbon dioxide had been eliminated. At a pressure of 0.2 GPa, the powdered material was further compressed into pellets that had an 8 mm diameter and a roughly 2 mm thickness. The sintering process comes next. Sintering was performed on the prepared pellet composition for four hours at 1450 °C. For the synthesized $(Ba_{1-x}Sr_xCa_{0.1})(Zr_{1-z}Ti_z)O_3$ (x = 0.20, z = 0.9) composition, the above mentioned sintering condition was chosen to achieve a respectable density (Roy P K et al.

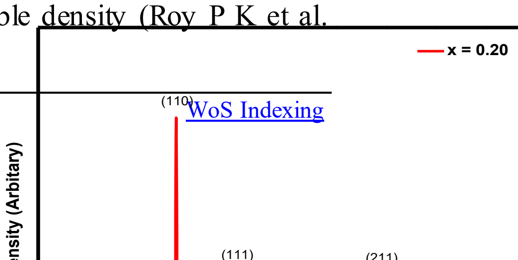

2017). The PANalytical X-ray diffractometer was utilized to measure the XRD patterns of the synthesized BSCZT pellet sample at room temperature. The measurement was taken at a wavelength of 1.54060 Å. With a step size of 0.02° and 0.3 sec per step, the X-ray diffraction measurements were taken over a wide range of 2θ (20° < 2θ < 70°). In order to investigate the dielectric and piezoelectric tests, conductive silver paste was used to electrode the composition in a metal-insulator-metal (MIM) configuration. A Keysight E49990 impedance analyzer was utilized to test the dielectric properties between RT and 450 °C. The tests were conducted in the frequency range of 12.74 to 1000 kHz. Using the EVO 18 Special Edition (CARL ZEISS), SEM pictures were examined to investigate the grain size and surface morphology. A piezometer installed inside a P-E loop tracer ("aixACCT Systems GmbH, aixPES") was used to measure the piezoelectric characteristics.

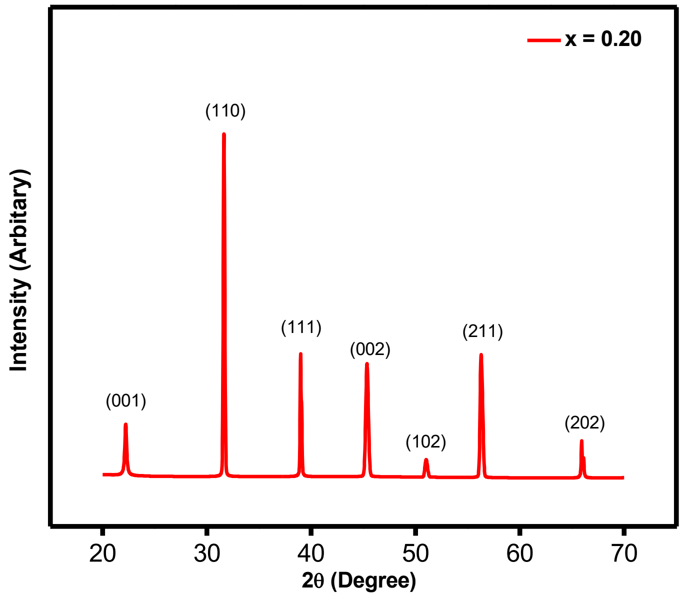

Fig. 1. XRD pattern of the prepared $(Ba_{1-x}Sr_xCa_{0.1})(Zr_{1-z}Ti_z)O_3$ (x = 0.20, z = 0.9) sample, in the 2θ range of 20-70°.

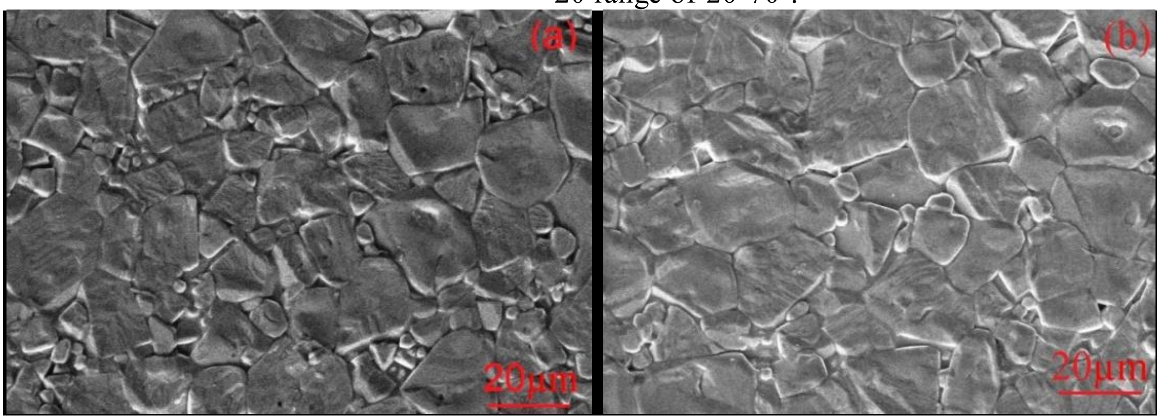

Fig. 2. Scanning electron microscopy pictures of $(Ba_{1-x}Sr_xCa_{0.1})(Zr_{1-z}Ti_z)O_3$ (x = 0.20, z = 0.9) composition.

 DOI: https://doi.org/10.51220/jmr.v21-S2.13

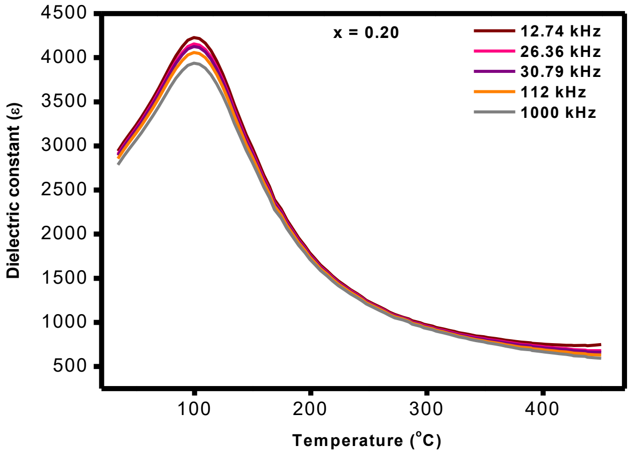

Fig. 3. Dielectric constant (ε) with the change in temperature for $(Ba_{1-x}Sr_xCa_{0.1})(Zr_{1-z}Ti_z)O_3$ (x = 0.20, z = 0.9) composition.

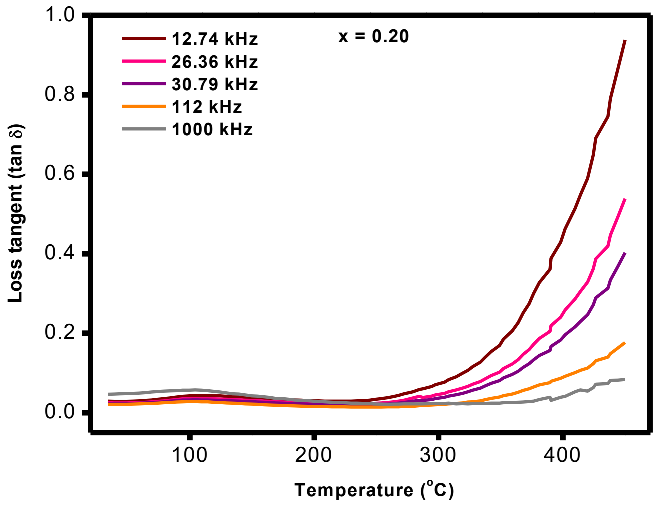

Fig. 4. Loss tangent (tan δ) with the change in temperature for $(Ba_{1-x}Sr_xCa_{0.1})(Zr_{1-z}Ti_z)O_3$ (x = 0.20, z = 0.9) composition

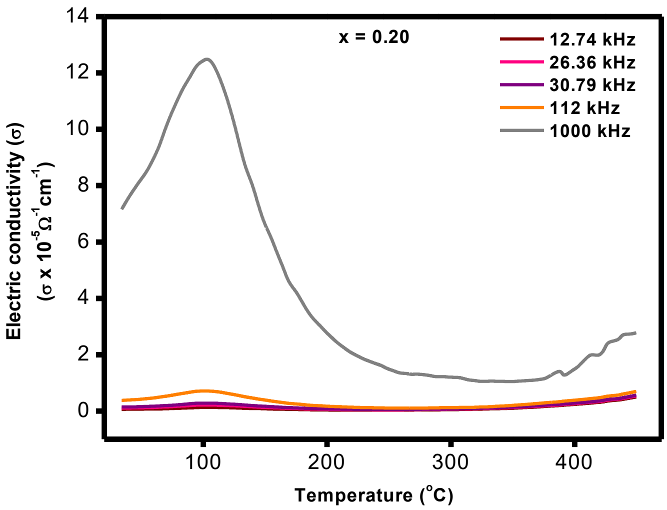

Fig. 5. Electric conductivity (*σ*) with the change in temperature for $(Ba_{1-x}Sr_xCa_{0.1})(Zr_{1-z}Ti_z)O_3$ (x = 0.20, z = 0.9) composition.

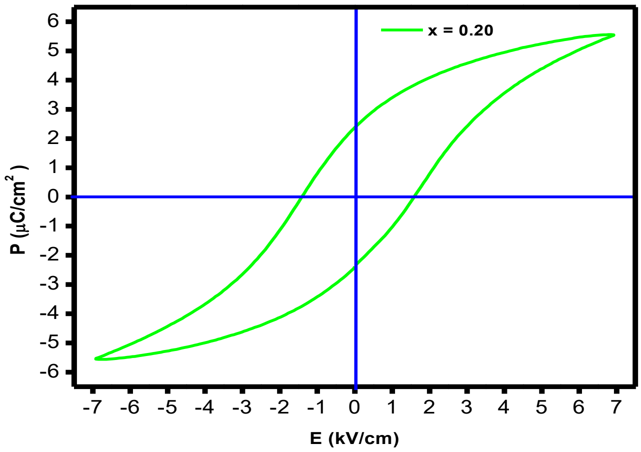

Fig. 6. (P-E) hysteresis loop of $(Ba_{1-x}Sr_xCa_{0.1})(Zr_{1-z}Ti_z)O_3$ (x = 0.20, z = 0.9) composition, at RT.

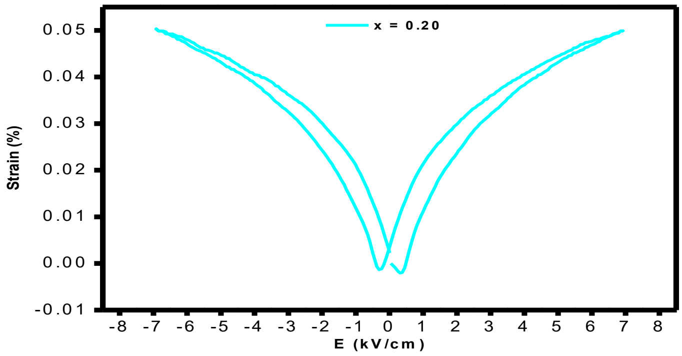

Fig. 7. Graph of S (%) vs. E of the prepared $(Ba_{1-x}Sr_xCa_{0.1})(Zr_{1-z}Ti_z)O_3$ (x = 0.20, z = 0.9) composition, at RT.

Results and discussion

XRD Measurements

X-ray diffraction pattern of the synthesized $(Ba_{1-x}Sr_xCa_{0.1})(Zr_{1-z}Ti_z)O_3$ (x = 0.20, z = 0.9) sample was taken at room temperature and shown in Figure 1. The pattern is in agreement with the ICSD data (01-079-2265) of the $(Ba_{1-x}Sr_xCa_{0.1})(Zr_{1-z}Ti_z)O_3$ (x = 0.20, z = 0.9) composition, which exhibit polycrystalline behavior with tetragonal symmetry. Peak indexing was done with the help of XRD data. Peaks similar to (001), (110), (111), and (002), are visible in the observed data of other researchers (Buttner R H et al., 1992). The diffraction pattern shows the pure, extra-phase-free ABO_3-type perovskite structure. High Score Plus software was utilized to carry out the Rietveld refinement process. The lattice constants and supplementary details of the $(Ba_{0.70}Sr_{0.20}Ca_{0.1})(Zr_{0.1}Ti_{0.9})O_3$ sample were computed with the help of this refinement (Table 1). Changes in lattice characteristics for BCZT compositions were also reported in a study by Biswas et al., demonstrating the impact of changing composition (x) (Biswas D et al. 2021). The composition exhibited the presence of the tetragonal structure with P4/mm space group at RT, as shown in Figure 1.

Table 1: Lattice constants and other specifications of the $(Ba_{1-x}Sr_xCa_{0.1})(Zr_{1-z}Ti_z)O_3$ (x = 0.20, z = 0.9) composition.

SL. No.	Specifications	Sample $(Ba_{1-x}Sr_xCa_{0.1})(Zr_{1-z}Ti_z)O_3$ (x = 0.20, z = 0.9)
1	a (Å)	4.008(3)
2	b (Å)	4.008(2)
3	c (Å)	4.017(3)
4	Space group	P4/mm
5	Bragg R	13.21

 DOI: https://doi.org/10.51220/jmr.v21-S2.13

SEM Measurements

The obtained SEM photographs of the synthesized $(Ba_{1-x}Sr_xCa_{0.1})(Zr_{1-z}Ti_z)O_3$ (x = 0.20, z = 0.9) composition are displayed in Figure 2. The average grain size of the BSCZT composition was around 8.5 µm. Additionally, it displays huge grains. The magnitude was determined by dividing the SEM photograph's length by the no. of grains it included. The prepared composition has well-developed uniform-grain properties, fine density, and homogeneity. The density of the sintered pellet sample was estimated utilizing the Archimedes technique. In general, there is a proportionate relationship between the density of the manufactured pellets and the grain size. In the current study, 4.7 gm/cm^3 is the computed density. It is important to remember that the BSCZT sample's dielectric properties are significantly influenced by both density and grain size (Kinoshita K et al., 1976, Hirata Y et al., 1996).

It was found that the density of the synthesized $(Ba_{1-x}Sr_xCa_{0.1})(Zr_{1-z}Ti_z)O_3$ (x = 0.20, z = 0.9) sample increased with the addition of Sr (x) (Biswas D et al. 2021, Roy P K, et al. 2017). The number of boundaries in samples is influenced by grain size; boundaries are less in larger grains and vice versa. Larger grains result in fewer grain boundaries in the composition of x = 0.20, which causes the synthesized BSCZT sample to become more polarized. The development of material grain, the character of free surfaces, the potential possibilities of grain boundaries, and the variation in the lattice structure can all be substantially impacted by the way sintering operates and the use of diverse methods. Dissimilar diffusion rates are caused by ions with dissimilar charges that are present in every diffusing species, regardless of volatility.

Dielectric Measurements

Temperature-dependent electric conductivity (σ), loss tangent (tan δ), and dielectric constant (ε) of the synthesized $(Ba_{1-x}Sr_xCa_{0.1})(Zr_{1-z}Ti_z)O_3$ (x = 0.20, z = 0.9) sample were measured at different frequencies between room temperature and 450 °C. The temperature-dependent dielectric characteristics ("ε, tan δ and σ") of the synthesized BSCZT ceramics are displayed in Figures 3, 4, and 5. For the aforementioned composition, the observed data indicated a rise in ε, tan δ, and σ for the prepared composition up to 100 °C as the temperature rose. The magnitudes were dropping after that temperature. The dielectric characteristics ("ε, tan δ, and σ") showed a clear peak value at approximately 100 °C at all measured frequencies.

At around 100 °C and 12.74 kHz, the maximum dielectric constant (ε = 4256) was recorded, but the electric conductivity (1.25 x $10^{-5}\Omega^{-1}cm^{-1}$) peaked at 1 MHz. The composition of the BSCZT ceramics had a major impact on their dielectric properties. However, the dielectric characteristics of the pellet samples are significantly influenced by the density, voids, porosity, microstructure, and grain size (Kinoshita K et al., 1976 , Frey M H et al., 1998). Furthermore, elements like internal stress and the existence of a liquid phase may have an impact on the dielectric behavior seen in BSCZT sample (Biswas D et al. 2021, Frey M H et al., 1998)

Piezoelectric Measurements

At room temperature, the (P-E) ferroelectric loop of the synthesized $(Ba_{1-x}Sr_xCa_{0.1})(Zr_{1-z}Ti_z)O_3$ (x = 0.20, z = 0.9) composition was obtained by applying a peak electric field (E) of 7 kV/cm and a triangle wave with a frequency of 1 Hz. The outcome is displayed in Figure 6. A significant ferroelectric nature was demonstrated by the synthesized $(Ba_{1-x}Sr_xCa_{0.1})(Zr_{1-z}Ti_z)O_3$ (x = 0.20, z = 0.9) sample. The coercive field (P_c = 1.60 kV/cm) and remnant polarization (P_r = 2.42 µC/cm^2) were determined for the aforementioned composition. Furthermore, Figure 7 illustrates the soft domain reorientation characteristics seen in the butterfly-like structures by showing the S(%) change with the applied E properties of the synthesized BSCZT composition (Viola G et al., 2013). Applying an electric field can alter the ferroelectric domain inside the synthesized ceramics. Furthermore, domain walls move in response to strain, piezoelectric effect, and electrostriction, resulting in a complicated nonlinear hysteresis character that is categorized by a strain-electric field loop that resembles to a butterfly (Viola G et al., 2013).

The strain (%) with the change in electric field (E) was computed for the synthesized $(Ba_{1-x}Sr_xCa_{0.1})(Zr_{1-z}Ti_z)O_3$ (x = 0.20, z = 0.9) composition, which is shown in Figure 7. The "piezoelectric constant (d_{33}^*)" was calculated by taking the ratio of highest strain (S_{max}) and electric field (E_{max}) (Jalalian A et al., 2014 Biswas D et al., 2022). The magnitudes of S_{max} and E_{max} were calculated from the butterfly plot (Figure 7) (Jalalian A et al., 2014 Biswas D et al., 2022). The composition with x = 0.20 exhibited a good "piezoelectric constant" (d_{33}^* = 724 pm/V). By altering the solid solution's composition and preparation circumstances, material qualities can frequently be controlled (McQuarrie M et al., 1954). The purity and grain size of the powder samples (Nalwa H S 1999) , as well as the processing parameters (Mitra S et al., 2013), have a considerable influence on the internal stress, flaws, and morphology of the ceramics. The prepared composition's crystalline structure, density, and grain size significantly affect its ferroelectric characteristics (Mudinepalli V R et al., 2015, Shen Z Y et al., 2010).

Conclusions

The $(Ba_{1-x}Sr_xCa_{0.1})(Zr_{1-z}Ti_z)O_3$ (x = 0.20, z = 0.9) composition was synthesized utilizing the solid-state reaction technique. At around 100 °C and across all frequencies, the composition shows the maximum magnitudes for the relative permittivity characteristics. The said composition provides good ferroelectric properties. For the synthesized composition, the obtained electrical properties may be selected as a potential feature for various sensor and transducer applications.

References

Bahri F, Khemakhem H (2014)., Raman and dielectric investigation of (Ba0.9-xSrxCa0.1)(Ti0.8Zr0.2)O3 ferroelectric ceramics, Ceram. Int. 40 (2014) 7909–7913. https://doi.org/10.1016/j.ceramint.2013.12.138

Biswas D, Sharma P, Panwar N S (2021)., Composition dependent electrical properties of $(Ba_{1-x}Ca_xZr_{0.1}Ti_{0.9})O_3$ ceramics, near morphotropic phase boundary (0.140 ≤ x ≤ 0.160), ECS J. Solid State Sci. Technol. 10 (2021) 033002. https://doi.org/10.1149/2162-8777/abea61

Biswas D, Sharma P, Panwar N S (2021)., Dielectric properties of $Na_{1-x}K_xNbO_3$ (NKN) (0.160 ≤ x ≤ 0.200) ceramics synthesized by double sintered method, Ferroelectrics. 571 (2021) 214–229. https://doi.org/10.1080/00150193.2020.1853757

Biswas D, Sharma P, Panwar N S (2021)., Structural and electrical properties of lead free $Na_{1-x}K_xNbO_3$ (0.160 ≤ x ≤ 0.200) ceramics, Ceram. Int. 47 (2021) 13814–13819. https://doi.org/10.1016/j.ceramint.2021.01.246

Biswas D, Sharma P, Panwar N S (2022)., Structural and piezoelectric properties of (Ba1-xCaxZr0.1Ti0.9)O3 ceramics, near morphotropic phase boundary (0.140 ≤ x ≤ 0.160), Indian J. Pure Appl. Phys. 60 (2022) 111–116. https://doi.org/10.56042/ijpap.v60i2.57525

Buttner R H, Maslen E N (1992)., Structural parameters and electron difference density in BaTiO3, Acta Crystallogr., Sect. B: Struct. Sci. 48 (1992) 764. https://doi.org/10.1107/S010876819200510X

Chao X, Wang J, Liang P, Zhang T, Wei L, Yang Z (2016)., Phase transition and

 DOI: https://doi.org/10.51220/jmr.v21-S2.13

improved electrical performance of $Ba_{0.85}Ca_{0.15}Zr_{0.1}Ti_{0.9}O_3$–$Ca_{0.28}Ba_{0.72}Nb_2O_6$ ceramics with high Curie temperature, Mater. Des. 89 (2016) 465–469. https://doi.org/10.1016/j.matdes.2015.10.014

Dawber M, Rabe K M, Scott J F (2005)., Physics of thin-film ferroelectric oxides, Rev. Mod. Phys. 77 (2005) 1083. https://doi.org/10.1103/RevModPhys.77.1083

Frey M H, Xu Z, Han P, Payne D A (1998)., The role of interfaces on an apparent grain size effect on the dielectric properties for ferroelectric barium titanate ceramics, Ferroelectrics. 206 (1998) 337–353. https://doi.org/10.1080/00150199808009168

Hirata Y, Nitta A, Sameshima S, Kamino Y (1996)., Dielectric properties of barium titanate prepared by hot isostatic pressing, Mater. Lett. 29 (1996) 229. https://doi.org/10.1016/S0167-577X(96)00149-8

Jalalian A, Grishin A M, Wang X L, Cheng Z X, Dou S X (2014)., Large piezoelectric coefficient and ferroelectric nanodomain switching in Ba $(Ti_{0.80}Zr_{0.20})$ O_3-$0.5(Ba_{0.70}Ca_{0.30})TiO_3$ nanofibers and thin films, Appl. Phys. Lett. 104 (2014) 103112. https://doi.org/10.1063/1.4867013

Jiang M, Lin Q, Lin D, Zheng Q, Fan X, Wu X, Sun H, Wan Y, Wu L (2013)., Effects of MnO_2 and sintering temperature on microstructure, ferroelectric, and piezoelectric properties of $Ba_{0.85}Ca_{0.15}Ti_{0.90}Zr_{0.10}O_3$ lead-free ceramics, J. Mater. Sci. 48 (2013) 1035–1041. https://doi.org/10.1007/s10853-012-6835-y

Kantha P, Pengpat K (2009)., Phase formation and electrical properties of BNLT–BZT lead-free piezoelectric ceramic system, Curr. Appl. Phys. 9 (2009) 460–466. https://doi.org/10.1016/j.cap.2008.04.004

Kim S, Choi H, Lee M, Park J, Kim D, Do D, Kim M, Song T, Kim W (2013)., Electrical properties and phase of BaTiO3–SrTiO3 solid solution, Ceram. Int. 39 (2013) S487–S490. https://doi.org/10.1016/j.ceramint.2012.10.119

Kinoshita K, Yamaji A (1976)., Grain-size effects on dielectric properties in barium titanate ceramics, J. Appl. Phys. 47 (1976) 371. https://doi.org/10.1063/1.322330

Liu X, Chen Z, Fang B, Ding J, Zhao X, Xu H, Luo H (2015)., Enhancing piezoelectric properties of BCZT ceramics by Sr and Sn co-doping, J. Alloys Compd. 640 (2015) 128–133. https://doi.org/10.1016/j.jallcom.2015.04.029

Maraj M, Wei W, Peng B, Sun W (2019)., Dielectric and energy storage properties of $Ba_{(1-x)}Ca_xZr_yTi_{(1-y)}O_3$ (BCZT): a review, Materials. 12 (2019) 3641. https://doi.org/10.3390/ma12213641

McQuarrie M, Behnke F W (1954)., Structural and dielectric studies in the system (Ba, Ca)(Ti, Zr)O_3, J. Am. Ceram. Soc. 37 (1954) 539–543.

Mitra S, Kulkarni A R, Prakash O (2013)., Diffuse phase transition and electrical properties of lead-free piezoelectric $(Li_xNa_{1-x})NbO_3$ ($0.04 \leq x \leq 0.20$) ceramics near morphotropic phase boundary, J. Appl. Phys. 114 (2013) 064106. https://doi.org/10.1063/1.4817815

Mudinepalli V R, Feng L, Lin W C, Murty B S (2015)., Effect of grain size on dielectric and ferroelectric properties of nanostructured $Ba_{0.8}Sr_{0.2}TiO_3$ ceramics, J. Adv. Ceramics. 4 (2015) 46–53. https://doi.org/10.1007/s40145-015-0130-8

Nalwa H S (1999)., Handbook of nanostructured materials and nanotechnology, 1st ed., Academic Press Publishing, New York.

DOI: https://doi.org/10.51220/jmr.v21-S2.13

Pisitpipathsin N, Kantha P, Pengpat K, Rujijanagul G (2013)., Influence of Ca substitution on microstructure and electrical properties of Ba(Zr,Ti)O3 ceramics, Ceram. Int. 39 (2013) S35–S39. https://doi.org/10.1016/j.ceramint.2012.10.031

Puli V S, Pradhan D K, Riggs B C, Adireddy S, Katiyar R S, Chrisey D B (2014)., Synthesis and characterization of lead-free ternary component BST-BCT-BZT ceramic capacitors, J. Adv. Dielectr. 4 (2014) 1450014. https://doi.org/10.1142/S2010135X14500143

Roy P K, Ponraj B, Varma K B R (2017)., Dielectric, ferroelectric and piezoelectric properties of (Ba0.98-xSrxCa0.02)(Ti0.95Zr0.05)O3 lead-free ceramics, Ceram. Int. 43 (2017) 15762–15768. http://dx.doi.org/10.1016/j.ceramint.2017.08.139

Saito Y, Takao H, Tani T, Nonoyama T, Takatori K, Homma T, Nagaya T, Nakamura M (2004)., Lead-free piezoceramics, Nature. 432 (2004) 84–87. https://doi.org/10.1038/nature03028

Samara G A (1987)., Effects of pressure on the dielectric properties and phase transitions of the alkali metal tantalates and niobates, Ferroelectrics. 73 (1987) 145–159. https://doi.org/10.1080/00150198708227914

Sateesh P, Omprakash J, Kumar G, Prasad G (2015)., Studies of phase transition and impedance behavior of Ba(Zr,Ti)O_3 ceramics, J. Adv. Dielectr. 5 (2015) 1550002. https://doi.org/10.1142/S2010135X15500022

Sen S, Choudhay R (2004)., Effect of doping Ca ions on structural and electrical properties of Ba(Zr0.05Ti0.95)O3 electroceramics, J. Mater. Sci.: Mater. Electron. 15 (2004) 671–675. https://doi.org/10.1023/B:JMSE.0000038922.74021.d6

Shen Z Y, Li J F (2010)., Enhancement of piezoelectric constant d_{33} in $BaTiO_3$ ceramics due to nano-domain structure, J. Ceram. Soc. Jpn. 118 (2010) 940–943. https://doi.org/10.2109/jcersj2.118.940

Srinivas A, Krishnaiah R, Niranjani V, Kamat S, Karthik T, Asthana S (2015)., Ferroelectric, piezoelectric and mechanical properties in lead free (0.5) $Ba(Zr_{0.2}Ti_{0.8})O_3$-(0.5)$(Ba_{0.7}Ca_{0.3})TiO_3$ electroceramics, Ceram. Int. 41 (2015) 1980–1985. https://doi.org/10.1016/j.ceramint.2014.08.127

Takenaka T, Nagata H (2005)., Current status and prospects of lead-free piezoelectric ceramics, J. Eur. Ceram. Soc. 25 (2005) 2693–2700. https://doi.org/10.1016/j.jeurceramsoc.2005.03.125

Viola G, Saunders T, Wei X, Chong K B, Luo H, Reece M J, Yan H (2013)., Contribution of piezoelectric effect, electrostriction and ferroelectric/ferroelastic switching to strain-electric field response of dielectrics, J. Adv. Dielectr. 3 (2013) 1350007. https://doi.org/10.1142/S2010135X13500070

Wu J, Xiao D, Wu B, Wu W, Zhu J, Yang Z, Wang J (2012)., Sintering temperature induced electrical properties of $(Ba_{0.90}Ca_{0.10})(Ti_{0.85}Zr_{0.15})O_3$ lead-free ceramics, Mater. Res. Bull. 47 (2012) 1281–1284. https://doi.org/10.1016/j.materresbull.2012.01.032